



North Pacific Fisheries Commission

NPFC-2023-SSC PS12-IP06

**The interannual to decadal relationship between total catch variability of Pacific saury
(*Cololabis saira*) and basin-scale ocean environmental variability in the North Pacific**

Jihwan Kim¹, Toshihide Kitakado², Robert Day¹, Aleksandr Zavolokin¹, and Rentaro Mitsuyu²

¹North Pacific Fisheries Commission, Tokyo, Japan

² Department of Marine Biosciences, Tokyo University of Marine Science and Technology,
Tokyo, Japan

*Corresponding author: Toshihide Kitakado (kitakado@kaiyodai.ac.jp)

Department of Marine Biosciences, Tokyo University of Marine Science and Technology, Tokyo
108-8477, Japan

Keywords: Pacific saury, North Pacific Gyre Oscillation, Kuroshio-Oyashio Extension, Kuroshio
Extension Jet, Oyashio Current, Sea of Okhotsk

Target Journal: *Scientific Reports*

Abstract

The Pacific saury is one of the keystone species in marine ecosystems of the North Pacific and is of great value to fisheries. Its fluctuating total annual catch and significant decline over the past decade underscore the importance of understanding the factors affecting its abundance, including its relationship to long-term ocean environmental variability. This study examined the relationship between annual Pacific saury catch and the North Pacific basin-scale ocean environment. The results show a significant correlation between increased catches and the intensification of the Kuroshio Extension jet. Increased biological productivity, as measured by net primary production, is evident in the Kuroshio-Oyashio extension region along with increased saury catches. This increase is associated with the warming of the Sea of Okhotsk and the intensification of both the Kuroshio Extension Jet and the Oyashio Current. A 2-year lead-lag relationship between the North Pacific Gyre Oscillation and saury catches suggests its potential as a predictor of annual catch amounts of Pacific saury abundance. These results may be used to improve the assessment of Pacific saury stocks and thereby contribute to sustainable fisheries management.

Introduction

The Pacific saury (*Cololabis saira*) is a species of considerable commercial importance including for China, Chinese Taipei, Japan, Republic of Korea, Russia, and Vanuatu^{1,2}. It has a wide distribution that spans the mid-latitude regions of the North Pacific³⁻⁵. Pacific saury is a short-lived species with a life span that varies between 1 and 2 years, making management of this stock a challenge^{2,6}.

The migratory patterns of Pacific saury include movements between the subtropical Kuroshio and the subarctic Oyashio, traversing the vast area known as the Kuroshio-Oyashio Transition Zone or Kuroshio-Oyashio Extension (KOE; 35–44° N, 141–175° E) (Figures 1a and 1b)^{7,8}. During the winter season, the spawning areas of Pacific saury are located in the south of Japan, recognized as the Kuroshio spawning area, while the feeding and fishing areas during the summer and fall seasons are mainly located around the northeast of Honshu (the main island of Japan) and the east of Hokkaido, recognized as the Oyashio feeding area^{1,4,8-13}. These seasonal movements and territorial preferences demonstrate the species' adaptive behavior and ecological tendencies and underscore its complex relationship with the various ocean conditions throughout its range^{1,4,12,13}.

Previous studies suggest that Pacific saury recruitment is significantly correlated with sea surface temperature (SST) and sea surface height (SSH) near the Kuroshio Current, as well as mixed layer depth within the KOE region^{5,9,10}. In addition, variables such as sea surface

chlorophyll, zooplankton, and net primary production (NPP) within the Oyashio Feeding Zone – components inherently linked to food resources – are strongly associated with Pacific saury recruitment^{14,15}. All of the oceanographic environmental factors that influence Pacific saury catch rates are related to the interactions and dynamics of the Kuroshio and Oyashio currents^{16–22}. For example, the southward extension of the Oyashio Current (offshore Oyashio Current and meanders) and the intensification of the Kuroshio Current along with the Kuroshio Extension (KE) jet (after the Kuroshio separates from the coast of Japan at approximately 35° N) are identified as important sources of biological productivity within the KOE region (Figures 1a–e)^{15,22–24}.

There are two dominant ocean environmental variabilities on interannual to decadal time scales in the North Pacific that influence the Kuroshio: the Pacific Decadal Oscillation (PDO) and the North Pacific Gyre Oscillation (NPGO)^{25,26}. The PDO, which is associated with the Aleutian Low, affects the strength of the Kuroshio and the meridional variability of the KOE, in particular the meridional shift of the KOE axis^{25,27–30}. The NPGO, which is associated with the North Pacific Oscillation, also affects the strength of the Kuroshio, although it influences the zonal KOE variability, which denotes the intensity of the KE jet^{26,31–34}. These variabilities modulate the KOE via large-scale oceanic adjustments of the SSH variability, driven by the Rossby wave propagation into the KOE region, about 2–3 years after the onset of PDO and NPGO events^{33,35,36}.

In recent years, catches of Pacific saury have declined significantly, a trend that has been observed both within the Exclusive Economic Zones of Japan and Russia, and also within the North Pacific Fisheries Commission (NPFC) Convention Area (Figure 1f)^{22,37-40}. There has been a great deal of scientific debate about the causes of this decline, with suggestions ranging from increased fishing mortality (e.g., through increases in the number of fishing vessels, fishing days, and catch per unit effort (CPUE)) to climate change, expressed as ocean warming and other large-scale climate variability³⁸⁻⁴⁰. However, the cause of the fluctuations of the Pacific saury catch remains unclear³⁸.

Given its significant economic importance and the implications for maximum sustainable yield under climate change, it is imperative to accurately determine whether Pacific saury abundance variability is a consequence of anthropogenic impacts, inherent natural variability, or both. A detailed study of the interaction between ocean environmental variability, with a focus on the strength of the Kuroshio and KE jets, and climatic variability, represented by the PDO and NPGO, may provide insights into the ocean conditions associated with the variability of Pacific saury productivity. In the broader context of basin-wide changes in ocean conditions, it may explain the observed Pacific saury catch variability in the Northwestern Pacific over the past decade.

This study examines the relationship between variability in Pacific saury catches within the Northwestern Pacific and variability in the ocean environment of the North Pacific, analyzed on

interannual to decadal time scales. In addition, the study uses statistical methods to identify the prevailing ocean conditions that correspond to periods of increased Pacific saury catches, thereby illuminating potential lead-lag relationships with basin-scale climate variability in the North Pacific. A detailed examination of lead-lag relationships between the catch amounts and basin-scale ocean conditions provides information on the observed recent declines in Pacific saury catches.

Results

Ocean conditions related to the Pacific saury catches

Figure 2 shows the regressed SST anomalies onto the annual catches of Pacific saury from the two different data sets – Northwestern Pacific (NWP) and North Pacific (NP) – and regressed PC time series with the annual catch amounts of Pacific saury during 1990–2020. The regressed SST anomalies show an overall surface cooling within the KOE region. This potentially indicates the southward extension of the Oyashio Current, accompanied by surface warming within the Sea of Okhotsk and eastward of approximately 160° E. The R-squared values for the regressed SST anomalies are 0.44 and 0.33, respectively, suggesting a slightly higher correlation of regional SST variability with Pacific saury catches compared to basin-scale SST variability. A notable observation, however, is that the anomalies exhibit similar spatial patterns despite the different regions (NWP and NP) they represent. These coherent spatial patterns of SST anomalies indicate

that Pacific saury catches are influenced not only by regional SST variability but also by large-scale SST variability at the basin scale. This suggests a possible connection between Pacific saury catch variability and large-scale environmental variability in the North Pacific. While SST can explain the variability in Pacific saury catches, the regression results for atmospheric environmental variables – temperature at 2 m, mean sea level pressure, and wind speed at 10 m – show statistical insignificance (not shown). The results suggest that Pacific saury catches are more strongly correlated with oceanic processes, such as upper ocean current variability, than with atmospheric processes, including upwelling and net heat flux – the critical air-sea energy exchange responsible for surface warming or cooling – which may have a direct influence on surface biological productivity.

Figure 3 shows the regressed SSH anomalies onto the annual catches of Pacific saury from the two different data sets – NWP and NP – and regressed PC time series with the annual catch amounts of Pacific saury during 1990–2020. The SSH anomalies derived from both data sets also show similar spatial patterns. These patterns show positive SSH anomalies in regions southwest of Japan and within the KE jet, and negative SSH anomalies south of Japan and north of the KE jet. This spatial pattern suggests an intensification of the Kuroshio current south of Japan and the KE jet. In addition, the monthly SSH anomalies show the origin of the positive SSH anomaly in the interior of the North Pacific, which may be indicative of Rossby wave propagation, although not explicitly shown here (not shown). Unlike the regressed SST anomalies, the R-squared value

for the SSH anomaly within the NP is superior to that within the NWP, suggesting a predominant relationship between basin-scale ocean processes and Pacific saury catches in the North Pacific region.

Figure 4 shows zonally averaged ($145\text{--}155^\circ\text{ E}$) regressed temperature and zonal current anomalies upper 300 m and regressed NPP anomaly upper 100 m onto the annual catch amounts of Pacific saury. From the surface to 300 m depth, anomalies in temperature and zonal currents show physically coherent spatial patterns with those of SSH anomaly. In particular, the weak subsurface warming south of 35° N and surface to subsurface cooling between $35\text{--}43^\circ\text{ N}$ illustrates an enhanced temperature gradient, implying a corresponding strengthening of the KE jet, as shown by the positive zonal current anomalies around 35° N . In addition, the temperature anomaly shows that the warming from the surface to near-surface regions (approximately 50 m depth) occurs mostly north of 43° N . From the surface to a depth of 100 meters, a positive anomaly in NPP could be observed generally north of 33° N . In simple terms, this means that there's an increase in the basic biological activity that supports the food chain, such as phytoplankton growth. Since the primary High seas fisheries operate in the $38\text{--}47^\circ\text{ N}$ latitude range, this increased biological productivity suggests that there may be an increase in catches of Pacific saury.

Figure 5 displays regressed temperature and current anomalies at 45 m depth and regressed NPP anomaly at 5 m depth onto the annual catch amounts of Pacific saury. Temperature and

current velocity anomalies at 45 m depth indicate near-surface warming in the southwestern part of the Sea of Okhotsk, near Hokkaido, and Pacific waters off the Kuril Islands. This warming is consistent with the surface to near-surface warming observed in the zonally averaged temperature anomaly approximately north of 43° N. The temperature anomaly shows a near-surface cooling east of Honshu and south of Hokkaido, accompanied by a prevailing westward current anomaly, highlighting the intensification of the Oyashio Current. The NPP anomaly shows a positive anomaly consistent with the zonally averaged NPP anomaly approximately north of 33° N. An increase in biological productivity, which can provide favorable ocean conditions for Pacific saury, is observed in the southwestern part of the Sea of Okhotsk, the Pacific waters of the Kuril Islands, the eastern coasts of Honshu and Hokkaido, and regions that include the High Seas Pacific saury fishery.

Relationship between the NPGO and Pacific saury catches

The observed correlation coefficients between Pacific saury catches and the annually averaged NPGO index reveal a statistically significant relationship when the NPGO precedes Pacific saury fluctuations by a span of 2 years, with $r = 0.51$, $p < .01$ during 1950–2020 (Supplementary figure 2). This indicates a potential temporal relationship wherein NPGO-related ocean environmental variability might be preceding Pacific saury catch fluctuations. In contrast,

correlations concerning the PDO do not demonstrate any statistically significant relationship (not shown).

Figure 6 displays SSH anomalies regressed onto the 2-year low-pass filtered NPGO index with lags. In the periods before 2 years and up to half a year after the onset of the positive phase of NPGO, SSH anomalies show a negative anomaly in the KE jet region and a positive anomaly north of the KE region. Such anomalies suggest a possible weakening of the KE jet. Beyond the six-month post-NPGO, the positive SSH anomaly appears to migrate southward, showing positive anomalies in the KE jet region. Over time, these SSH anomalies become increasingly positive, while areas north of the KE jet region show negative anomalies. Such temporal evolutions suggest an increase in the strength of the KE jet following the NPGO event.

Notably, the SSH anomaly in the KE jet region shows a positive anomaly after the onset of the NPGO. Part of this positive anomaly appears to originate from the eastern regions, mainly the interior of the North Pacific, suggesting a westward propagation of the Rossby wave associated with the NPGO. Remarkably, two years after the NPGO event, the SSH anomaly reflects spatial patterns comparable to those observed during the increase in the Pacific saury catches, characterized by positive SSH anomalies in the KE jet region and negative anomalies north of the KE jet. These results may indicate a temporal relationship connecting Pacific saury catch variability to basin-scale ocean environmental variability, exemplified by the NPGO.

The regressed ocean environmental variables such as SST, SSH, upper ocean temperature and current velocity, and NPP, suggest a potential increase in Pacific saury catches under ocean conditions characterized by the intensification of the KE jet, the warming of the southwestern part of Sea of Okhotsk, the strengthening of the Oyashio Current, and the corresponding increase in biological productivity within the KOE region and regions the southwestern part of Sea of Okhotsk. This includes the Pacific waters off the Kuril Islands, which has been identified as a major fishing area for Pacific saury. The Ocean environmental variability associated with the NPGO, characterized by a 2-year lag, shows similar environmental variability to that of the Pacific saury, the intensified KE jet, which significantly impacts biological productivity in the KOE (Figures 3 and 6). This similarity is consistent with the observed lead-lag correlation between Pacific saury catches and the annually averaged NPGO index. Thus, the results may indicate a possible lead-lag relationship between Pacific saury catches and basin-scale ocean processes associated with the NPGO.

Discussion

Ocean conditions in the period of high productivity of stock

Regressed SSH, temperature, and zonal current velocity anomalies onto the annual catch amounts of Pacific saury illustrate the enhanced KE jet; positive SSH anomaly in the KE jet region and enhanced meridional temperature gradients around 35° N with positive zonal current

velocity anomaly (Figures 2–5). Previous studies suggest that a stronger Kuroshio current, including the KE jet, facilitates the influx of greater quantities of zooplankton into the KOE region^{41,42}. This influx, in turn, amplifies biological productivity. This abundance of zooplankton increases biological productivity in the KOE region and may contribute to an overall enhancement of ecological conditions within the KOE region, potentially establishing more favorable ocean conditions conducive to the Pacific saury stock^{43–46}. Therefore, the regressed ocean environmental variables suggest the role of the Kuroshio Current in influencing favorable ocean conditions for the Pacific saury fishery, which is mainly caught in the KOE region^{14,15,22–24}.

The regressed SST and temperature anomalies observed at 45 m depth show a surface to near-surface cooling off of the eastern and northeastern coasts of Japan (Figures 2 and 5). This surface to near-surface cooling may indicate the potential intensification of the Oyashio Current. It is noteworthy to consider this in the context of increased catches of Pacific saury in the region. The surface to near-surface cooling, consistent with previous studies, suggests a positive correlation between the strengthening of the Oyashio Current and increased catches of Pacific saury^{42,47–50}. This relationship may be attributed to the role of the Oyashio Current in transporting nutrient-rich waters from northern latitudes to coastal areas such as those near Japan. As a result, changes in the southward extent and intensified of the Oyashio Current may significantly affect the annual catch amounts of Pacific saury^{22,40}.

Regressed vertical temperature and NPP anomalies suggest that when Pacific saury catches increase, the southwestern part of the Sea of Okhotsk shows surface to near-surface warming with positive NPP anomaly near the main fishing grounds of Pacific saury (Figure 4). Specifically, an increase in Pacific saury catches corresponds to the surface to near-surface warming of the southwestern part of the Sea of Okhotsk and Pacific waters off the Kuril Islands, accompanied by a positive NPP anomaly, indicating increased biological productivity in the primary Pacific saury fishing grounds (Figures 4 and 5). These results suggest a robust link between temperature variations within the Sea of Okhotsk and corresponding variations in NPP, a connection that is directly relevant to facilitating favorable conditions for Pacific saury catches^{47,51-54}.

Furthermore, an examination of monthly temperature and NPP anomalies reveals that the presence of a positive NPP anomaly in the southwestern part of the Sea of Okhotsk, as well as near Hokkaido and Pacific waters off the Kuril Islands, corresponds to the onset of surface to near-surface warming within the Sea of Okhotsk, which typically begins in the summer season (Supplementary figures 3 and 4). This climatic effect reinforces the favorable environment necessary for the proliferation of Pacific saury. Thus, the interplay of factors, including the intensity of the KE jet, the Oyashio Current, and the temperature dynamics that characterize the Sea of Okhotsk, collectively emerge as key determinants influencing the variability observed in Pacific saury catches.

Relationship between the NPGO and the Pacific saury catches

The increase in temperature in the southwestern part of the Sea of Okhotsk corresponds to an increase in the catch amount of Pacific saury, which is not observed after a two-year lag of the positive phase of NPGO (Supplementary figures 5 and 6). However, the regression of surface to near-surface NPP on the two-year lagged NPGO reveals a biologically productive ocean condition around the southwestern part of the Sea of Okhotsk and the Hokkaido the fishing grounds for Pacific saury (Supplementary figures 7 and 8). While the enhanced surface to near-surface NPP is not associated with the temperature-related NPP increase of the Sea of Okhotsk, that observed in the two-year lagged NPGO is associated with the westward Rossby wave propagation. These are linked to ocean environmental variability, the strength of the KE jet, and the total zooplankton flux along with the mixed layer depth in the KOE region.^{41,43–45}

Previous studies have suggested that about 2–3 years after the positive phase of the NPGO events, the KE jet is enhanced by the westward Rossby wave propagation^{31,33–36}. They also emphasize that during periods of enhanced KE jet, there is an increase in zooplankton flux transported by the Kuroshio current within the KOE region^{41,42}. This increase in zooplankton flux can result in conditions that support abundant Pacific saury catches. Post-NPGO conditions include SSH anomalies, which show mostly weak negative anomalies in the KOE region and near the coasts of Hokkaido and the Pacific waters off the Kuril Islands, coupled with cooling of surface-to-subsurface. These SSH and temperature anomalies may indicate a shallow mixed layer

depth in the KOE region, which not only provides a biologically favorable environment for Pacific saury but also causes their movement to the near-surface due to fisheries exploiting the shallow mixed layer depth^{41,44,45}. In conclusion, the results of this study reveal a basin-scale lead-lag relationship between Pacific saury catches and the NPGO, characterized by a two-year lag, highlighting the complex interactions and consequent impacts on marine life and their respective ecosystems.

While the NPGO shows a lead-lag relationship with the total Pacific saury catch, the PDO does not show a statistically significant relationship, possibly due to their different effects on the Kuroshio. Previous studies suggest a link between the PDO and KOE meridional variability, reflecting the meridional shift of the KE jet^{27,29,30}. In contrast, the NPGO is associated with the zonal variability of the KOE, reflecting the strength of the KE jet. The strength of the KE jet is more relevant to zooplankton variability in the KOE region than the meridional shift of the KE jet itself³¹⁻³³. Therefore, the intensification of the KE jet attributed to the NPGO could potentially lead to increased zooplankton transport into the KOE region⁴¹. In contrast, the ocean environmental variability associated with the PDO does not induce significant changes in zooplankton variability within the KOE region. Furthermore, the regressed SSH, vertical temperature and NPP anomalies associated with the PDO show contrasting spatial patterns to those associated with the NPGO (Supplementary figures 9–11). This contrast may elucidate a

possible lead-lag relationship between the NPGO and Pacific saury catches, a relationship not evident with the PDO.

Concluding remarks

This study suggests that observed variations in Pacific saury catches on interannual to decadal scales are not exclusively correlated with local ocean processes. This also indicates a possible connection between the Pacific saury catches and basin-scale ocean environmental variability, primarily the NPGO with a 2-year lag. This relationship indicates a potential predictability of Pacific saury abundance in the North Pacific. It also suggests that the notable decline in the total catch of Pacific saury in the Northwestern Pacific in recent years may be influenced by natural ocean variability, including variability associated with the negative phase of the NPGO. While this interpretation is based on the data and analyses presented in the study, it is important to clarify that the results do not exclude the possible role of anthropogenic impacts, such as overfishing. Overfishing and Illegal, Unreported and unregulated (IUU) fishing continue to pose a challenge on the high seas, affecting both conservation and research efforts. Therefore, consistent monitoring of fishing activities, along with continued conservation and research, remains essential. It should be noted that the interpretations in this study should not be construed as an official position or opinion of the NPFC.

This study is limited by its sole reliance on the total catch of Pacific saury in the Northwestern Pacific and does not use the CPUE even if they exhibit similar variabilities. To avoid the potential effects of human activities, such as changes in the number of fishing vessels and fishing gear, only post-1990 data were used. However, the results of the study indicate that fluctuating ocean conditions (natural variability) are likely to be the primary drivers of the variation in catch levels. This suggests that human impacts (anthropogenic effects) may have had less of a role from 1990 to 2020 compared to the influence of ocean variability (natural variability). Future studies incorporating CPUE data are recommended for a more comprehensive understanding of fishery-related variability in ocean conditions.

Data and Method

Fisheries Data

This study uses annual catch data for Pacific saury in the Northwestern Pacific, including North Pacific Fisheries Commission (NPFC) Convention Area, from 1995 to 2022³⁷. In this study, catch amounts are used as an indicator of stock abundance. The underlying assumption is based on the probabilistic relationship that increased stock abundance is likely to result in increased catch amounts. The annual catch data show similar variability to the catch per unit effort (CPUE, in metric tons per operating day fished) using the vector autoregressive space-time model during the same period (not shown). The consistency between CPUE trends and observed total catch amounts variability supports the validity of catch amounts as an estimator of abundance.

In addition, data reported by the Food and Agriculture Organization of the United Nations (FAO) for the northwestern, northeastern, and eastern central Pacific Ocean between 1950 and 1994 are included to understand the long-term variability of Pacific saury catches in the Convention Area. The total catch of Pacific saury includes data reported by NPFC members: China, Chinese Taipei, Japan, Republic of Korea, Russia, and Vanuatu. Total catch data from the NPFC show consistent variability with data reported by the FAO from 1995 to 2014 (not shown), suggesting that FAO data before 1995 can be included in the NPFC dataset. To account for potential anthropogenic influences such as increases in the number of vessels, fishing days, vessel size variability, and advances in fishing gear, this study focuses only on fishery data after 1990 to

examine the interannual to decadal variability of Pacific saury catches about ocean environmental variability.

Ocean Environmental Variables

Monthly mean temperature and current velocity of the upper 300 m depth and sea surface height (SSH) data during 1988–2020 were obtained from Simple Ocean Data Assimilation (SODA) 3.4.2, which has a spatial resolution of 0.5° ⁵⁵. Monthly Sea Surface Temperature (SST) data from 1988–2020 with a spatial resolution of 0.25° were obtained from the NOAA Optimum Interpolation SST v2.1⁵⁶. ERA5 monthly 2 m height temperature, sea surface pressure, and 10 m height wind velocity with 0.25° spatial resolution during 1988–2020 from the European Centre for Medium Range Weather Forecasts were used to understand the relationship between atmospheric variability and Pacific saury catches⁵⁷. Monthly net primary production (NPP) data in the upper 300 m depth during 1993–2020 were obtained, to understand biological productivity, at a resolution of 0.25° from the Global Ocean Biogeochemistry Hindcast provided by the Copernicus Marine Environment Monitoring System Service⁵⁸. The North Pacific Gyre Oscillation (NPGO) index and the Pacific Decadal Oscillation (PDO) index were used during 1950–2022.

To examine the lead-lag relationship between Pacific saury catches and the ocean environment in the context of basin-scale variability, this study introduced time lags of 1 or 2 yr.

This study also used datasets from multiple time periods: 1988–2016, 1989–2017, 1991–2019, and 1992–2020. This approach allowed a detailed examination of the temporal relationship between Pacific saury catches and climate indices. To understand the annual catch amounts of Pacific saury associated with regional and basin-scale ocean environmental variability, this study used two regions of the data set: Northwestern Pacific (NWP; 30–55° N, 130–175° E) and North Pacific (NP; 0–60° N, 120° E–120° W). In order to understand the variability of the ocean environment around the main fishing area for Pacific saury, ocean variables are presented only in the NWP.

Cyclostationary Empirical Orthogonal Function (CSEOF)

In this study, a cyclostationary empirical orthogonal function (CSEOF) analysis was conducted to extract the spatio-temporal variability of these geophysical variables including SST, SSH, temperature, current velocity, NPP, air temperature at 2 m height, mean sea level pressure, and 10 m height wind velocity^{59,60}. The CSEOF method has been utilized by various studies to investigate the relationship between a specific time series and the physical variability of the environmental variables^{61–63}. The geophysical variables, $G(r, t)$, are decomposed into cyclostationary loading vectors (CSLVs), $A_n(r, t)$ and their corresponding principal component (PC) time series, $B_n(t)$ as in Eq. (1):

$$G(r, t) = \sum_n A_n(r, t)B_n(t), \quad (1)$$

where n , r , and t denote the mode number, 2-dimensional space, and time, respectively. The current velocity and 10 m height wind velocity were analyzed as a single variable by combining both the zonal and meridional components. The CSEOF analysis was conducted separately on each environmental variable at each depth, and the CSLVs were obtained to demonstrate the physical evolution of environmental variables over a nested period d of 12 months. The n th mode of the CSLVs is expressed with periodicity d , as in Eq. (2):

$$A_n(r, t) = A_n(r, t + d) \quad (2)$$

Thus, $A_n(r, t)$ consists of 12 monthly spatial patterns that illustrate the spatio-temporal evolution of the n th mode. Its corresponding PC time series, $B_n(t)$, illustrates the temporal variation of the n th mode of spatial variation. Each of the PC time series is statistically independent and the CSLVs are perpendicular to one another.

Regression Analysis

The statistical relationship between the annual total catches of Pacific saury variability in the Convention Area of NPFC, $F(t)$, and ocean environmental variability was obtained by conducting regression analysis in the CSEOF space, as described by Eq. (3):

$$F(t) \approx \sum_{m=1}^{10} \alpha_m \tilde{B}_m(t), \quad (3)$$

where m denotes the mode number, α_m is the regression coefficient, and $\tilde{B}_m(t)$ is annually averaged the PC time series of each ocean environmental variable. Through the regression coefficient, α_m , the regressed and reconstructed ocean environmental variability, $R(r, t)$, can be obtained as in Eq. (4):

$$R(r, t) = \sum_{m=1}^{10} \alpha_m A_m(r, t) \quad (4)$$

Thus, the resulting physical evolutions of the ocean environment, $R(r, t)$, share the long-term variability of the fishery data, $F(t)$, with some regression error. Therefore, regressed environmental variables show the environmental conditions during an increase in Pacific saury catches. In this study, the first ten CSEOF PC time series of the predictors were used for the regression analysis to minimize the chance of overfitting, which can lead to unstable

predictability. The R-squared values of the regression are shown in Supplementary Figure 1. The R-squared values suggest that the ocean environmental variables exhibit statistically significant (above e-fold) explanatory power. In order to study the interannual to decadal relationship between the Pacific saury catches and the ocean conditions, the annual mean spatial patterns of $R(r, t)$ are presented.

The correlation between variations in the ocean environment and both PDO and NPGO was investigated using analogous regression analysis, but the analysis involved the monthly PC time series of the environmental variables because the PDO and NPGO indices are monthly available. The ocean environmental variables regressed on the indices represent ocean conditions during the positive phase of each index. Several lagged regression analyses were performed on the NPGO and PDO indices with time lags such as ± 1 year (e.g., between 1989–2017 and 1991–2019) and ± 2 years (e.g., between 1988–2016 and 1992–2020).

Data Availability Statement

The published article, together with the supplementary information accompanying it, contains all the data collected or evaluated in the course of this study. If further details are required, they can be obtained from the corresponding author upon reasoned request.

References

1. NPFC. 8th Meeting of the Small Scientific Committee on Pacific Saury Report NPFC-2021-SSC PS08-Final Report. (NPFC, 2021).
2. Hubbs, C. Revision of the sauries (Pisces, Scomberesocidae) with descriptions of two new genera and one new species. *Fish. Bull.* **77**, 521–566 (1980).
3. Fukushima, S. Synoptic analysis of migration and fishing conditions of Pacific saury in the northwest Pacific Ocean. *Tohoku Reg Fish Res Lab* **41**, 1–70 (1979).
4. Huang, W.-B. Comparisons of monthly and geographical variations in abundance and size composition of Pacific saury between the high-seas and coastal fishing grounds in the northwestern Pacific. *Fish. Sci.* **76**, 21–31 (2010).
5. Miyamoto, H. *et al.* Geographic variation in feeding of Pacific saury *Cololabis saira* in June and July in the North Pacific Ocean. *Fish. Oceanogr.* **29**, 558–571 (2020).
6. Huang, W.-B. & Huang, Y.-C. Maturity characteristics of pacific saury during fishing season in the Northwest Pacific. *J. Mar. Sci. Technol.* **23**, 27 (2015).
7. Kosaka, S. Life history of Pacific saury *Cololabis saira* in the Northwest Pacific and consideration of resource fluctuation based on it. *Bull. Tohoku Nat. Fish. Res. Inst.* **63**, 1–95 (2000).
8. Suyama, S. Study on the age, growth, and maturation process of Pacific saury *Cololabis saira* (Brevoort) in the North Pacific. *Bull. Fish. Res. Agen.* **5**, 68–113 (2002).

9. Watanabe, K., Tanaka, E., Yamada, S. & Kitakado, T. Spatial and temporal migration modeling for stock of Pacific saury *Cololabis saira* (Brevoort), incorporating effect of sea surface temperature. *Fish. Sci.* **72**, 1153–1165 (2006).
10. Watanabe, Y., Kurita, Y., Noto, M., Oozeki, Y. & Kitagawa, D. Growth and survival of Pacific saury *Cololabis saira* in the Kuroshio-Oyashio transitional waters. *J. Oceanogr.* **59**, 403–414 (2003).
11. Watanabe, Y. & Lo, N. C. Larval Production and Mortality of Pacific Saury, *Cololabis saira*, in the Northwestern Pacific Ocean¹. *Collected Reprints* **2**, 555 (1993).
12. Kurita, Y. Regional and interannual variations in spawning activity of Pacific saury *Cololabis saira* during northward migration in spring in the north-western Pacific. *J. Fish. Biol.* **69**, 846–859 (2006).
13. Kuroda, H. & Yokouchi, K. Interdecadal decrease in potential fishing areas for Pacific saury off the southeastern coast of Hokkaido, Japan. *Fish. Oceanogr.* **26**, 439–454 (2017).
14. Humston, R., Ault, J. S., Lutcavage, M. & Olson, D. B. Schooling and migration of large pelagic fishes relative to environmental cues. *Fish. Oceanogr.* **9**, 136–146 (2000).
15. ITO, S. I. *et al.* Initial design for a fish bioenergetics model of Pacific saury coupled to a lower trophic ecosystem model. *Fish. Oceanogr.* **13**, 111–124 (2004).

16. Ichii, T. *et al.* Oceanographic factors affecting interannual recruitment variability of Pacific saury (*Cololabis saira*) in the central and western North Pacific. *Fish. Oceanogr.* **27**, 445–457 (2018).
17. Liu, S. *et al.* Effects of oceanographic environment on the distribution and migration of Pacific saury (*Cololabis saira*) during main fishing season. *Sci. REP-UK* **12**, 13585 (2022).
18. Oozeki, Y., Watanabe, Y. & Kitagawa, D. Environmental factors affecting larval growth of Pacific saury, *Cololabis saira*, in the northwestern Pacific Ocean. *Fish. Oceanogr.* **13**, 44–53 (2004).
19. Tian, Y., Akamine, T. & Suda, M. Variations in the abundance of Pacific saury (*Cololabis saira*) from the northwestern Pacific in relation to oceanic-climate changes. *Fish. Res.* **60**, 439–454 (2003).
20. Tseng, C.-T. *et al.* Spatial and temporal variability of the Pacific saury (*Cololabis saira*) distribution in the northwestern Pacific Ocean. *ICES J. Mar. Sci.* **70**, 991–999 (2013).
21. Yatsu, A. & Watanabe, K. Effects of environmental factors on long-term population fluctuations and a recent decline of stock abundance of Pacific saury in the waters of northern Japan. *Fisheries Management Department of the Tohoku National Fisheries Research Institute, FRA, Hachinohe* (2017).
22. 研究・教育機構, 国. サンマの不漁要因解明について (調査・研究の進捗) 令和5年4月. (国立研究開発法人水 研究・教育機構, 2023).

23. Beaugrand, G., Reid, P. C., Ibanez, F., Lindley, J. A. & Edwards, M. Reorganization of North Atlantic marine copepod biodiversity and climate. *Science* **296**, 1692–1694 (2002).
24. Miller, A. J. & Schneider, N. Interdecadal climate regime dynamics in the North Pacific Ocean: Theories, observations and ecosystem impacts. *Prog. Oceanogr.* **47**, 355–379 (2000).
25. Mantua, N. J. & Hare, S. R. The Pacific decadal oscillation. *J. Oceanogr.* **58**, 35–44 (2002).
26. Di Lorenzo, E. *et al.* North Pacific Gyre Oscillation links ocean climate and ecosystem change. *Geophys. Res. Lett.* **35** (2008).
27. Andres, M. *et al.* Manifestation of the Pacific decadal oscillation in the Kuroshio. *Geophys. Res. Lett.* **36** (2009).
28. Qiu, B. Kuroshio Extension variability and forcing of the Pacific decadal oscillations: Responses and potential feedback. *J. Phys. Oceanogr.* **33**, 2465–2482 (2003).
29. Qiu, B., Schneider, N. & Chen, S. Coupled decadal variability in the North Pacific: An observationally constrained idealized model. *J. Clim.* **20**, 3602–3620 (2007).
30. Trenberth, K. & Hurrell, J. Decadal coupled atmosphere ocean variations in the North Pacific Ocean. *Canadian Special Publication of Fisheries and Aquatic Sciences*, 15–24 (1995).
31. Ceballos, L. I., Di Lorenzo, E., Hoyos, C. D., Schneider, N. & Taguchi, B. North Pacific Gyre Oscillation synchronizes climate fluctuations in the eastern and western boundary systems. *J. Clim.* **22**, 5163–5174 (2009).

32. Chhak, K. C., Di Lorenzo, E., Schneider, N. & Cummins, P. F. Forcing of low-frequency ocean variability in the northeast Pacific. *J. Clim.* **22**, 1255–1276 (2009).
33. Di Lorenzo, E. *et al.* Synthesis of Pacific Ocean climate and ecosystem dynamics. *Oceanogr.* **26**, 68–81 (2013).
34. Seager, R., Kushnir, Y., Naik, N. H., Cane, M. A. & Miller, J. Wind-driven shifts in the latitude of the Kuroshio–Oyashio Extension and generation of SST anomalies on decadal timescales. *J. Clim.* **14**, 4249–4265 (2001).
35. Sasaki, Y. N., Minobe, S. & Schneider, N. Decadal response of the Kuroshio Extension jet to Rossby waves: Observation and thin-jet theory. *J. Phys. Oceanogr.* **43**, 442–456 (2013).
36. Taguchi, B. *et al.* Decadal variability of the Kuroshio Extension: Observations and an eddy-resolving model hindcast. *J. Clim.* **20**, 2357–2377 (2007).
37. NPFC. 10th Meeting of the Small Scientific Committee on Pacific Saury REPORT NPFC-SSC PS10-Report. (NPFC, 2022).
38. NPFC. 11th Meeting of the Small Scientific Committee on Pacific Saury Report NPFC-2023-SSC PS11-Provisional Agenda. (NPFC, 2023).
39. NPFC. 3rd intersessional meeting of the Small Scientific Committee on Pacific Saury NPFC-2023-SSC PS11-RP03. (NPFC, 2023).
40. 水産研究・教育機構, 国. 2023 年度 サンマ長期漁海況予報 (国立研究開発法人 水産研究・教育機構, 2023).

41. Chiba, S. *et al.* Large-scale climate control of zooplankton transport and biogeography in the Kuroshio-Oyashio Extension region. *Geophys. Res. Lett.* **40**, 5182–5187 (2013).
42. Chiba, S., Sugisaki, H., Nonaka, M. & Saino, T. Geographical shift of zooplankton communities and decadal dynamics of the Kuroshio–Oyashio currents in the western North Pacific. *Glob. Change Biol.* **15**, 1846–1858 (2009).
43. Nonaka, M., Nakamura, H., Tanimoto, Y., Kagimoto, T. & Sasaki, H. Decadal variability in the Kuroshio–Oyashio Extension simulated in an eddy-resolving OGCM. *J. Clim.* **19**, 1970–1989 (2006).
44. Ohno, Y., Iwasaka, N., Kobashi, F. & Sato, Y. Mixed layer depth climatology of the North Pacific based on Argo observations. *J. Oceanogr.* **65**, 1–16 (2009).
45. Yasuda, I. Hydrographic structure and variability in the Kuroshio-Oyashio transition area. *J. Oceanogr.* **59**, 389–402 (2003).
46. Yasuda, I. & Watanabe, T. Chlorophyll a variation in the Kuroshio Extension revealed with a mixed-layer tracking float: Implication on the long-term change of Pacific saury (*Cololabis saira*). *Fish. Oceanogr.* **16**, 482–488 (2007).
47. Ikeda, T., Shiga, N. & Yamaguchi, A. Structure, biomass distribution and trophodynamics of the pelagic ecosystem in the Oyashio region, western subarctic Pacific. *J. Oceanogr.* **64**, 339–354 (2008).

48. Saito, H., Tsuda, A. & Kasai, H. Nutrient and plankton dynamics in the Oyashio region of the western subarctic Pacific Ocean. *Deep Sea Res. Part II Top. Stud. Oceanogr.* **49**, 5463–5486 (2002).
49. Tseng, C.-T. *et al.* Sea surface temperature fronts affect distribution of Pacific saury (*Cololabis saira*) in the Northwestern Pacific Ocean. *Deep Sea Res. Part II Top. Stud. Oceanogr.* **107**, 15–21 (2014).
50. Yasuda, I. & Watanabe, Y. On the relationship between the Oyashio front and saury fishing grounds in the north-western Pacific: a forecasting method for fishing ground locations. *Fish. Oceanogr.* **3**, 172–181 (1994).
51. Kim, S. T. A review of the Sea of Okhotsk ecosystem response to the climate with special emphasis on fish populations. *ICES J. Mar. Sci.* **69**, 1123–1133 (2012).
52. Kishi, S. *et al.* The prominent spring bloom and its relation to sea-ice melt in the Sea of Okhotsk, revealed by profiling floats. *Geophys. Res. Lett.* **48**, e2020GL091394 (2021).
53. Mustapha, M. A. & Saitoh, S.-I. Observations of sea ice interannual variations and spring bloom occurrences at the Japanese scallop farming area in the Okhotsk Sea using satellite imageries. *Estuar. Coast. Shelf Sci.* **77**, 577–588 (2008).
54. Sorokin, Y. I. & Sorokin, P. Y. Production in the Sea of Okhotsk. *J. Plankton. Res.* **21** (1999).
55. Carton, J. A. & Giese, B. S. A reanalysis of ocean climate using Simple Ocean Data Assimilation (SODA). *Mon. Weather. Rev.* **136**, 2999–3017 (2008).

56. Reynolds, R. W., Rayner, N. A., Smith, T. M., Stokes, D. C. & Wang, W. An improved in situ and satellite SST analysis for climate. *J. Clim.* **15**, 1609–1625 (2002).
57. Hersbach, H. *et al.* The ERA5 global reanalysis. *Q. J. Roy. Meteor. Soc.* **146**, 1999–2049 (2020).
58. Global Ocean Biogeochemistry Hindcast (ed Marine Data Store (MDS) E.U Copernicus Marine Service Information (CMEMS)).
59. Kim, K.-Y. & North, G. R. EOFs of harmonizable cyclostationary processes. *J. Atmos. Sci.* **54**, 2416–2427 (1997).
60. Kim, K.-Y., North, G. R. & Huang, J. EOFs of one-dimensional cyclostationary time series: Computations, examples, and stochastic modeling. *J. Atmos. Sci.* **53**, 1007–1017 (1996).
61. Kim, J. & Na, H. Interannual Variability of Yellowfin Tuna (*Thunnus albacares*) and Bigeye Tuna (*Thunnus obesus*) Catches in the Southwestern Tropical Indian Ocean and Its Relationship to Climate Variability. *Front. Mar. Sci.* **9**, 857405 (2022).
62. Kim, J., Na, H., Park, Y.-G. & Kim, Y. H. Potential predictability of skipjack tuna (*Katsuwonus pelamis*) catches in the Western Central Pacific. *Sci. REP-UK* **10**, 3193 (2020).
63. Kim, K.-Y., Hamlington, B. & Na, H. Theoretical foundation of cyclostationary EOF analysis for geophysical and climatic variables: concepts and examples. *EARTH-SCI. Rev.* **150**, 201–218 (2015).

Acknowledgements

The authors appreciate the contributions of all NPFC members in collecting and verifying Pacific saury catch data.

Author contributions

JK conducted the analysis, prepared the figures, and wrote the manuscript. JK designed the research and JK, TK, RD, AZ, and RM discussed the results. All authors contributed to the article and approved the submitted version.

Competing Interests

The authors declare no competing interests.

Figure Set

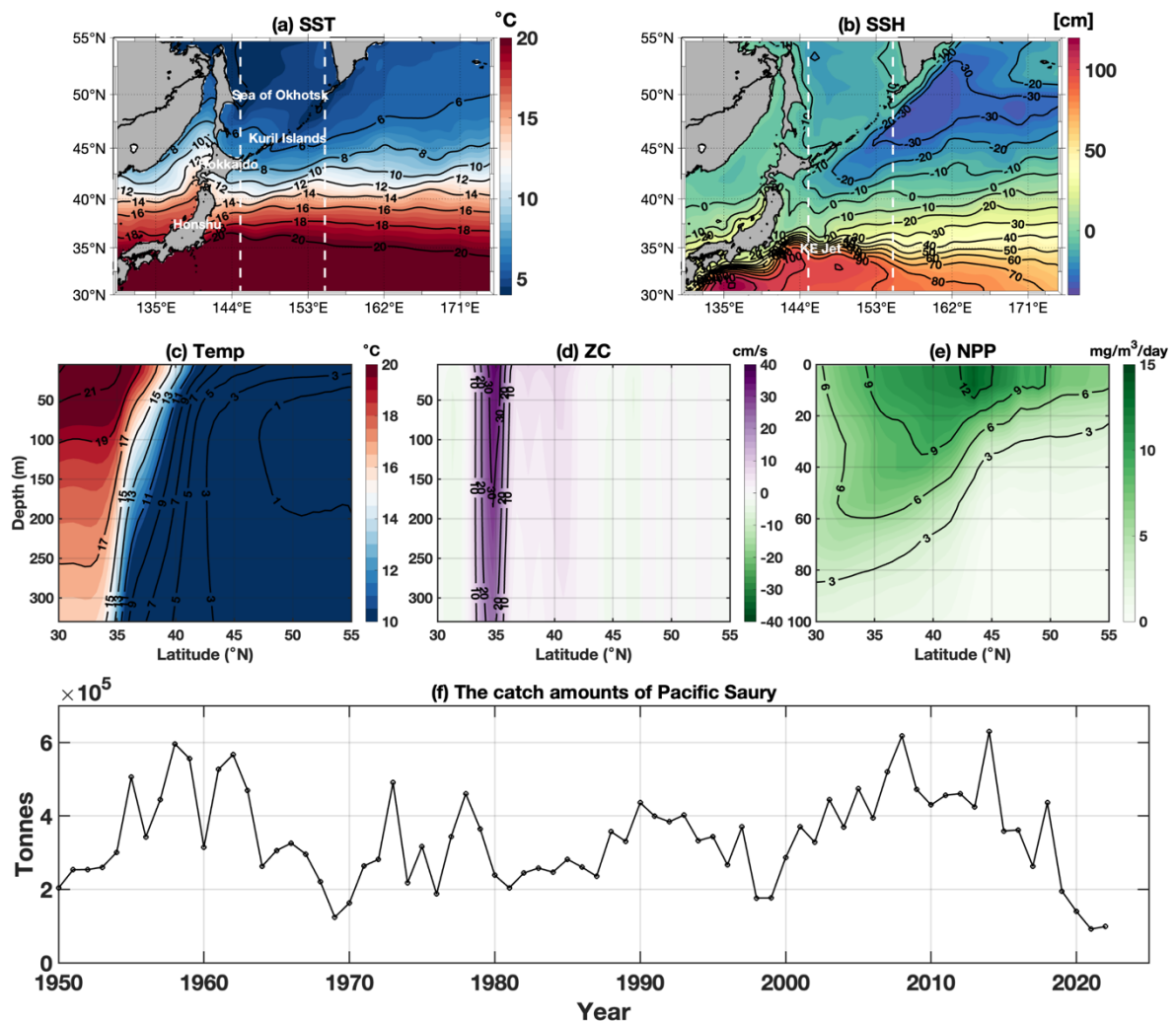


Figure 1. The mean ocean environmental variables and Pacific saury catches: (a) sea surface temperature (SST), (b) sea surface height (SSH), (c–e) zonally averaged (145–155° E) upper 300 m temperature (Temp) and zonal current velocity (ZC) accompanied by upper 100 m net primary production (NPP) from 1990–2020, except for NPP which is from 1993–2020, and (f) the annual catch amounts of Pacific saury in the Convention Area of North Pacific Fisheries Commission from 1950–2022. The vertical white dashed lines in the SST and SSH indicate the range of 145–155° E.

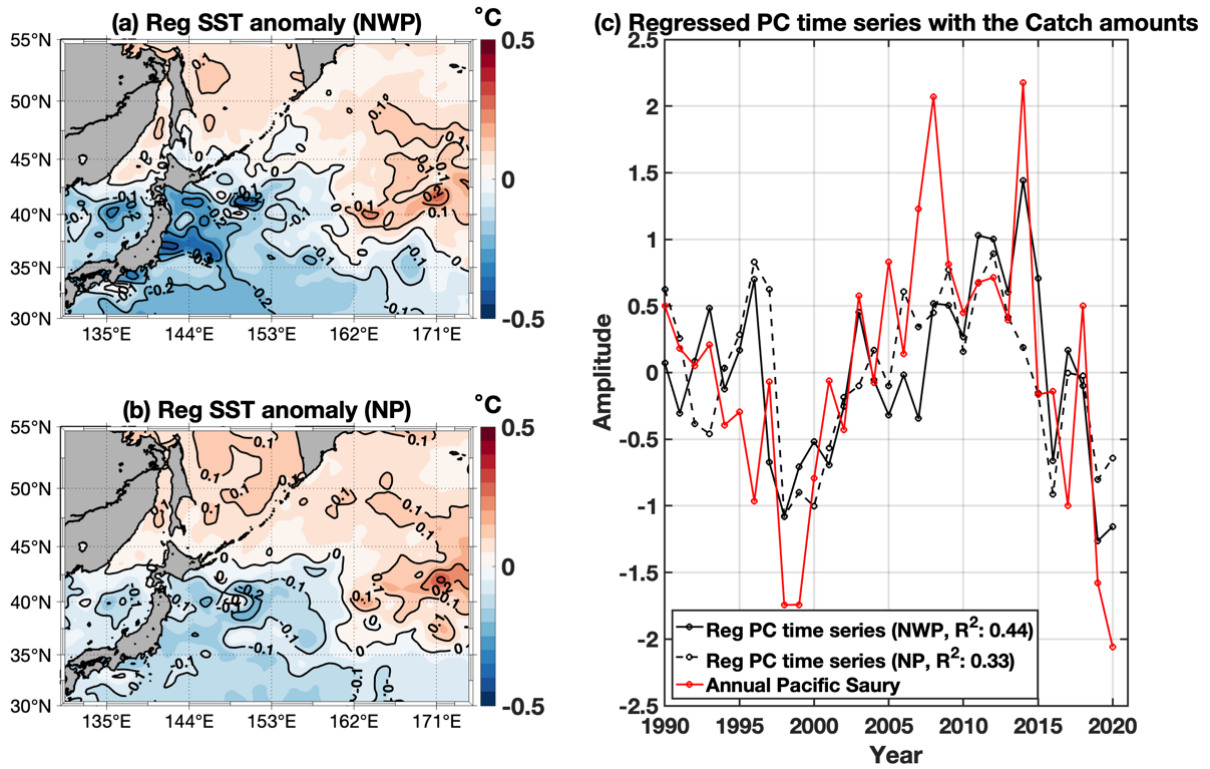


Figure 2. (a–b) The regressed and reconstructed sea surface temperature (SST) anomalies of the Northwestern Pacific (NWP) and North Pacific (NP) onto the annual catch amounts of Pacific saury during 1990–2020, respectively. (c) The regressed PC time series of the SST anomalies of the NWP and NP (black solid and black dashed lines, respectively) and the normalized annual catch amounts of Pacific saury (red solid line), during the same period.

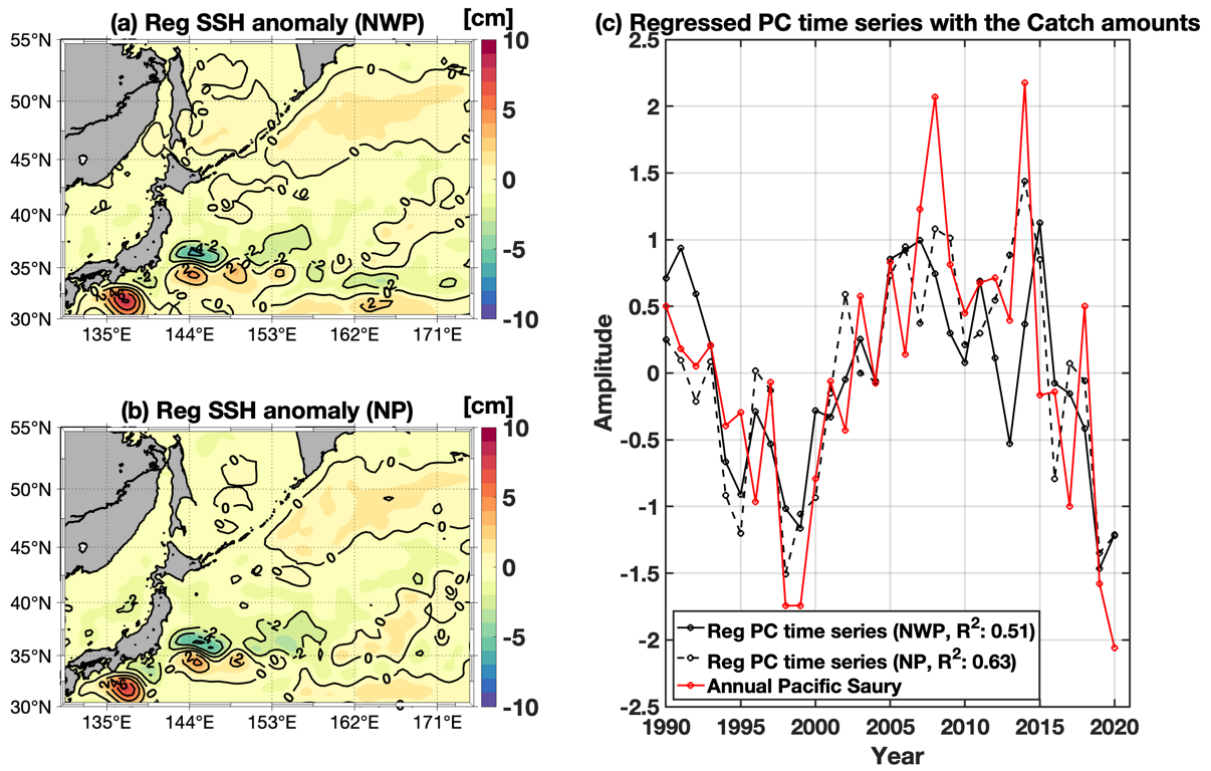


Figure 3. same as Figure 2, but for the sea surface height (SSH).

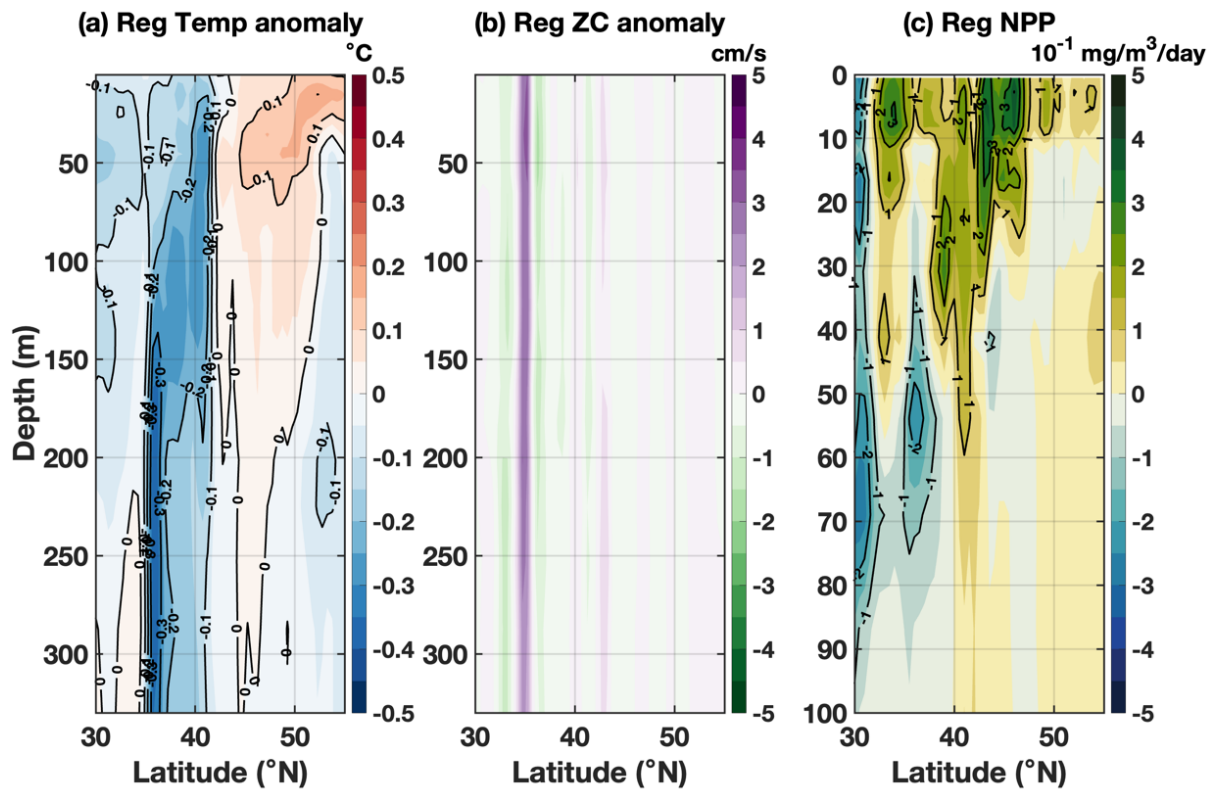


Figure 4. The zonally averaged ($145\text{--}155^{\circ}$ E) of the regressed and reconstructed anomalies of the ocean environmental variables in the North Pacific onto the annual catch amounts of Pacific saury during 1990–2020 (except for the net primary production (NPP) during 1993–2020): (left) upper 300 m temperature, (middle) upper 300 m zonal current velocity (ZC), and (right) upper 100 m NPP.

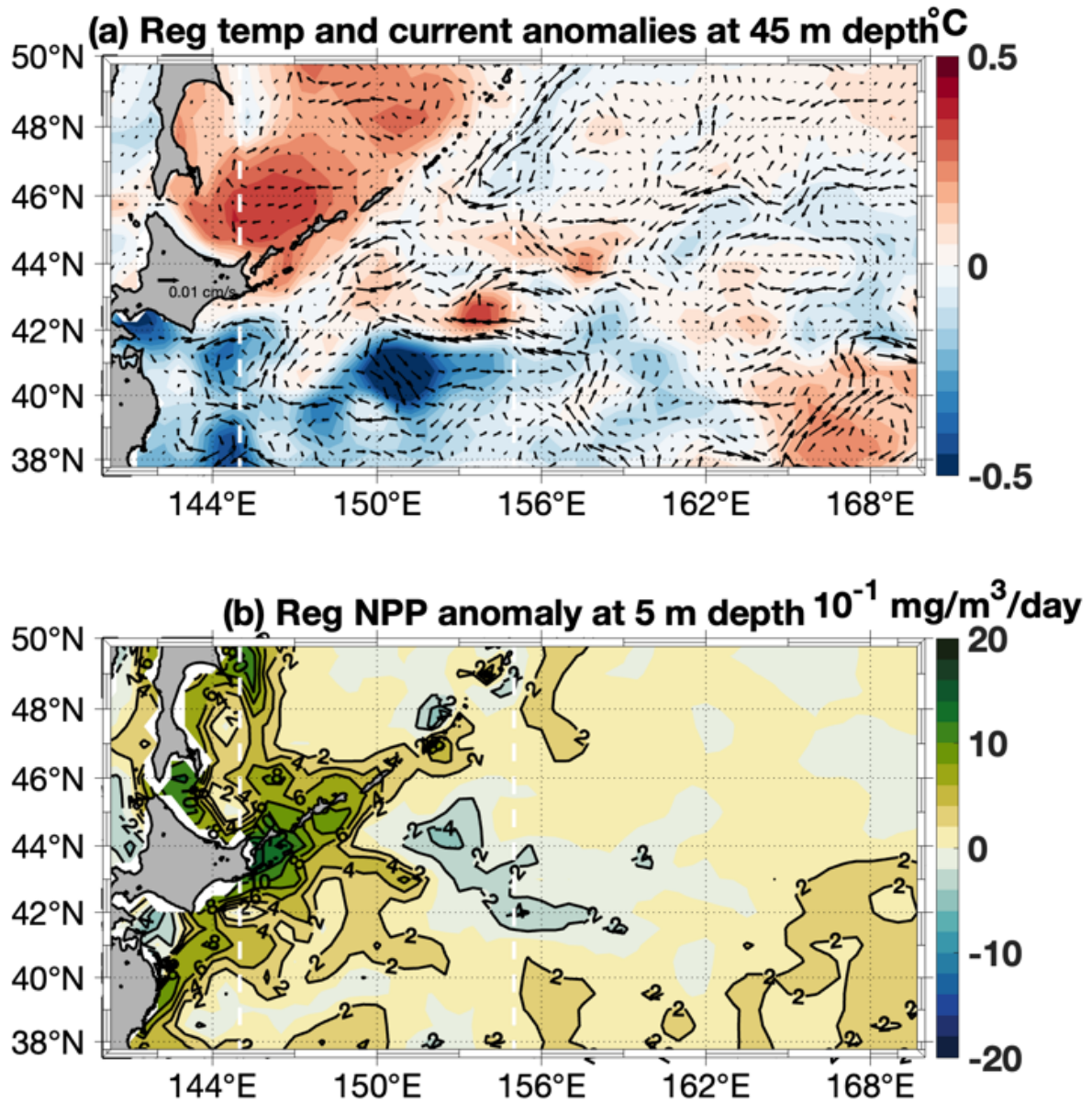


Figure 5. The regressed and reconstructed temperature and current at 45 m depth anomalies (top) and net primary production (NPP) anomaly at 5 m depth (bottom) in the North Pacific onto the annual catch amounts of Pacific saury during 1990–2020 (except for the NPP during 1993–2020), respectively. The vertical white dashed lines indicate the range of 145–155° E.

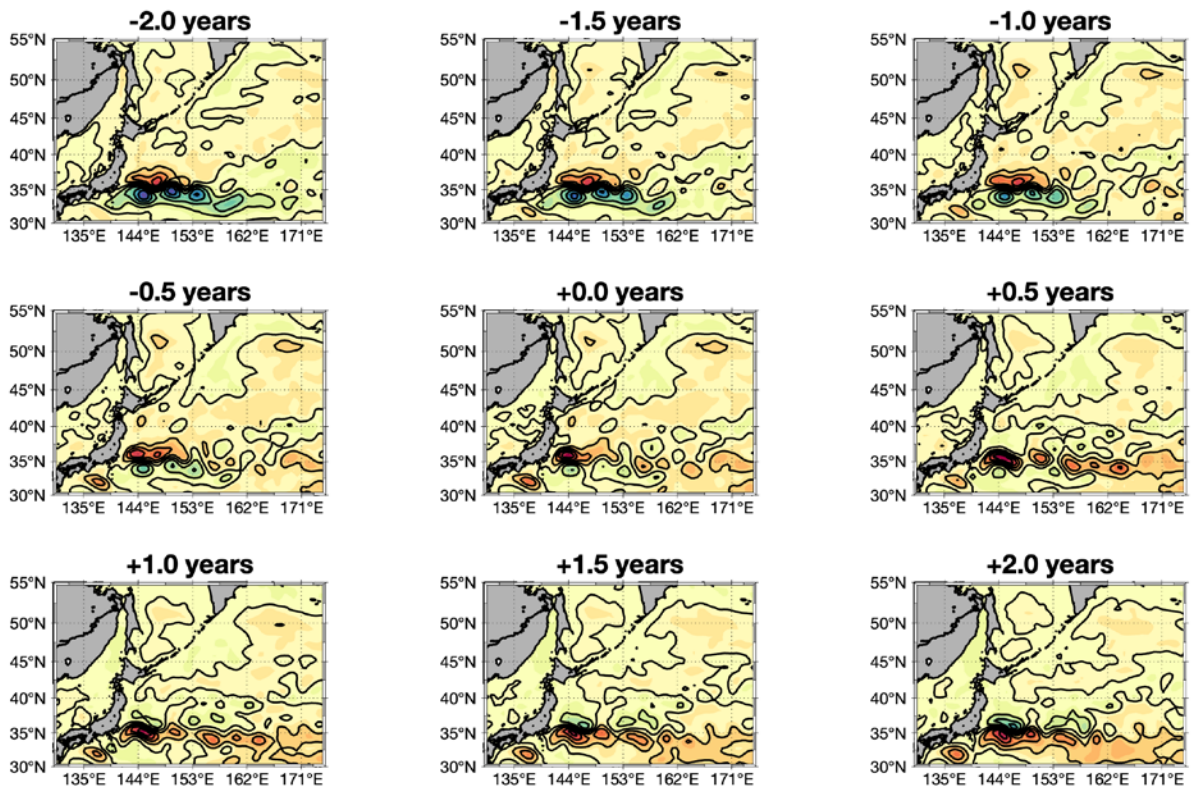
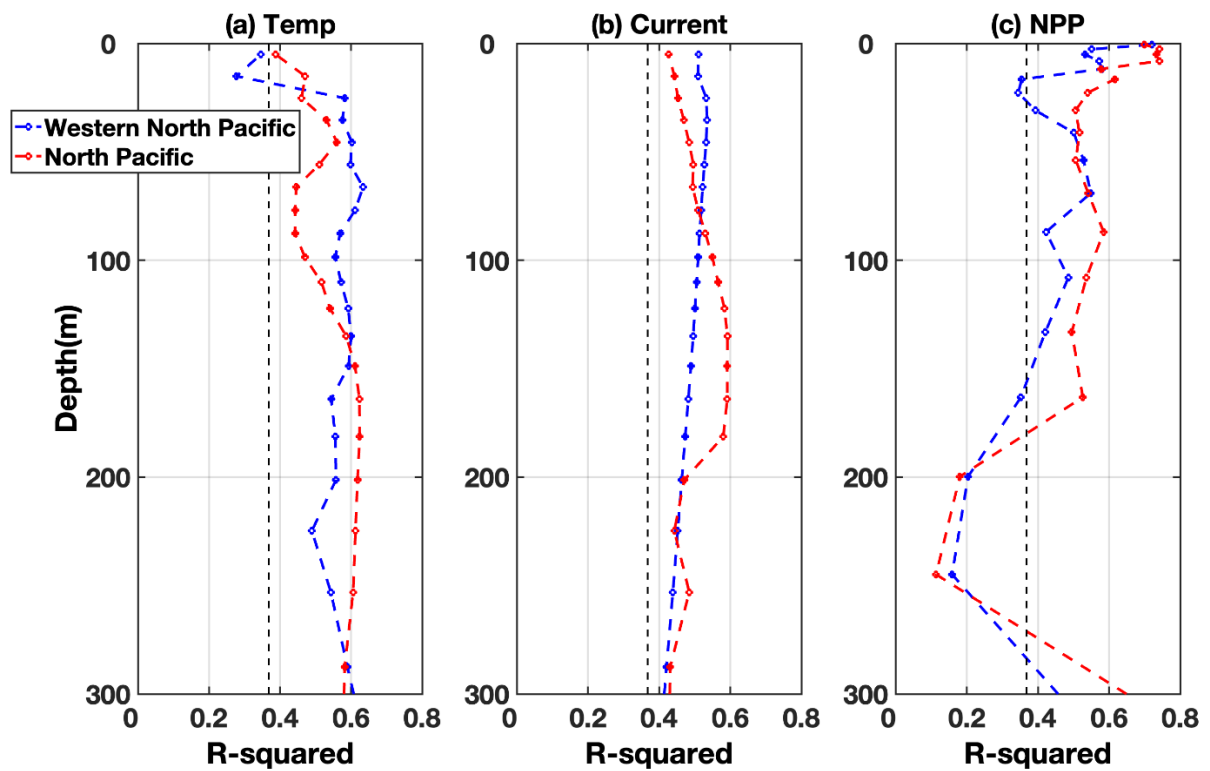
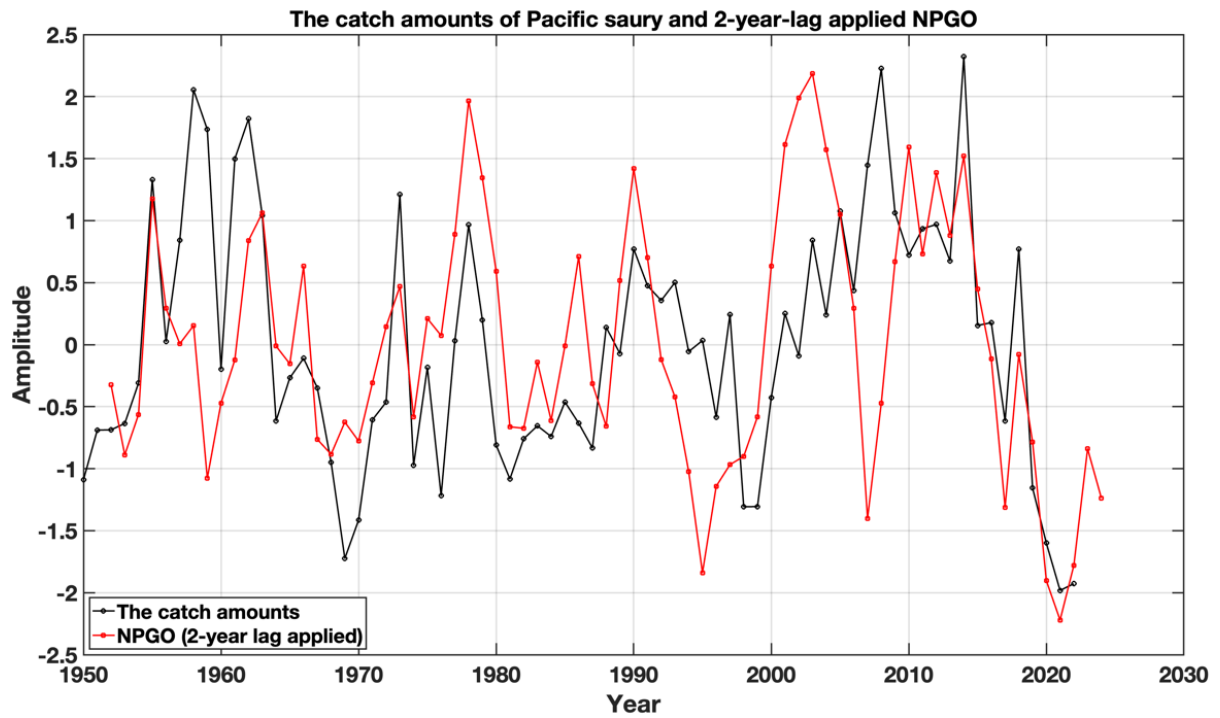


Figure 6. The regressed and reconstructed sea surface height (SSH) anomalies in the North Pacific onto the normalized 2-year low-pass filtered North Pacific Gyre Oscillation (NPGO) index (contour intervals: 2 cm). The target index is for 1990–2018, and the SSH anomalies are for 1988–2020, with a time lag of ± 2 years. Numbers in the title indicate the time lags and positive values indicate that the NPGO leads the SSH. Areas of positive SSH anomalies are shaded red, and areas of negative anomalies are shaded blue.

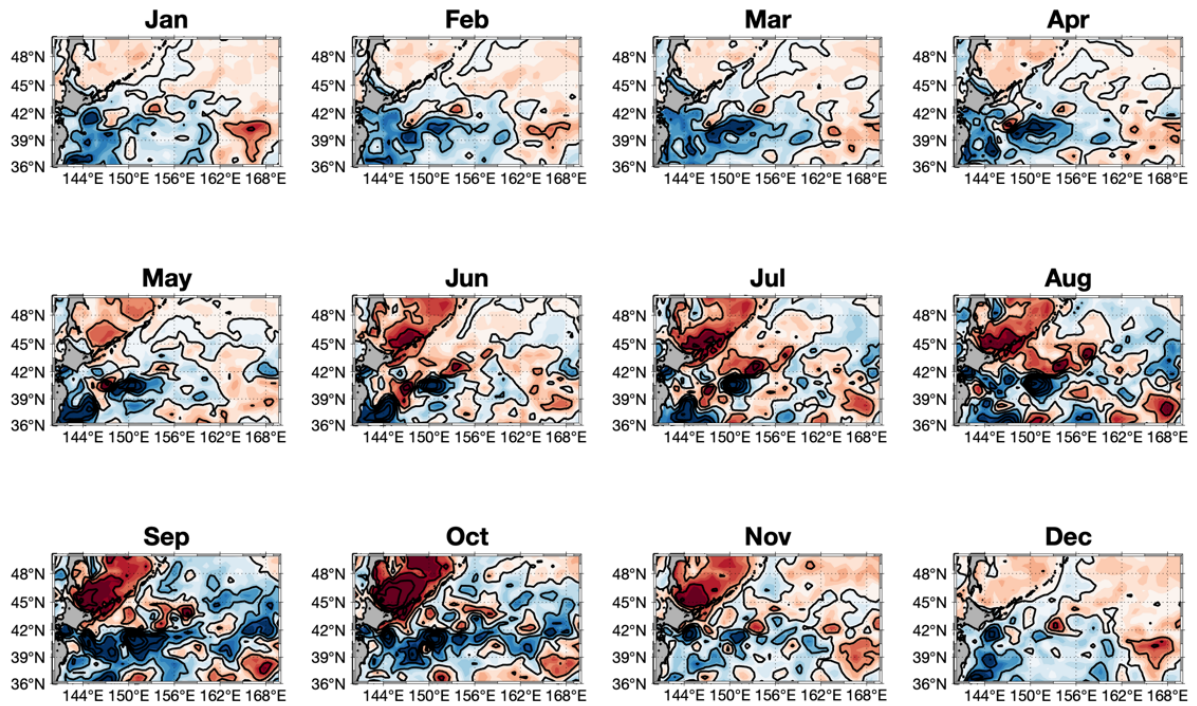
Supplementary figure set



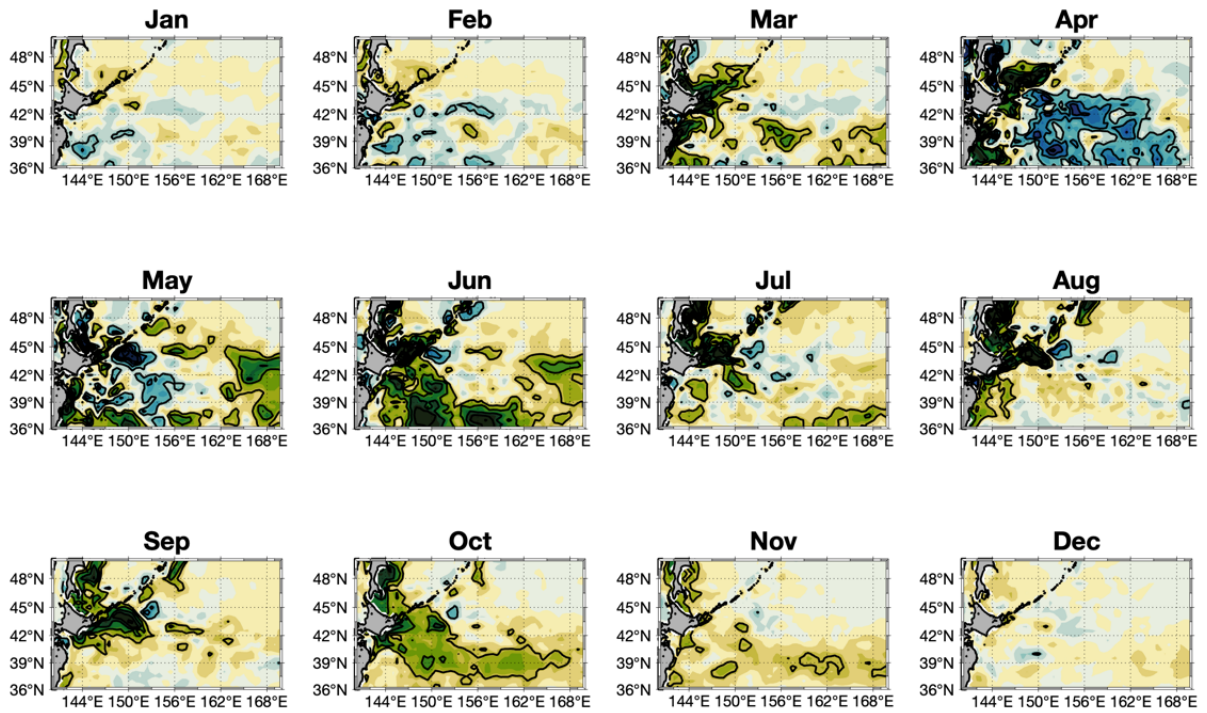
Supplementary figure 1. The R-squared values of the regression at each depth onto the annual catch amounts of Pacific saury during 1990–2020 (except for net primary production (NPP) during 1993–2020) for (a) temperature, (b) current velocity, and (c) NPP. The vertical dashed lines denote the e-folding value.



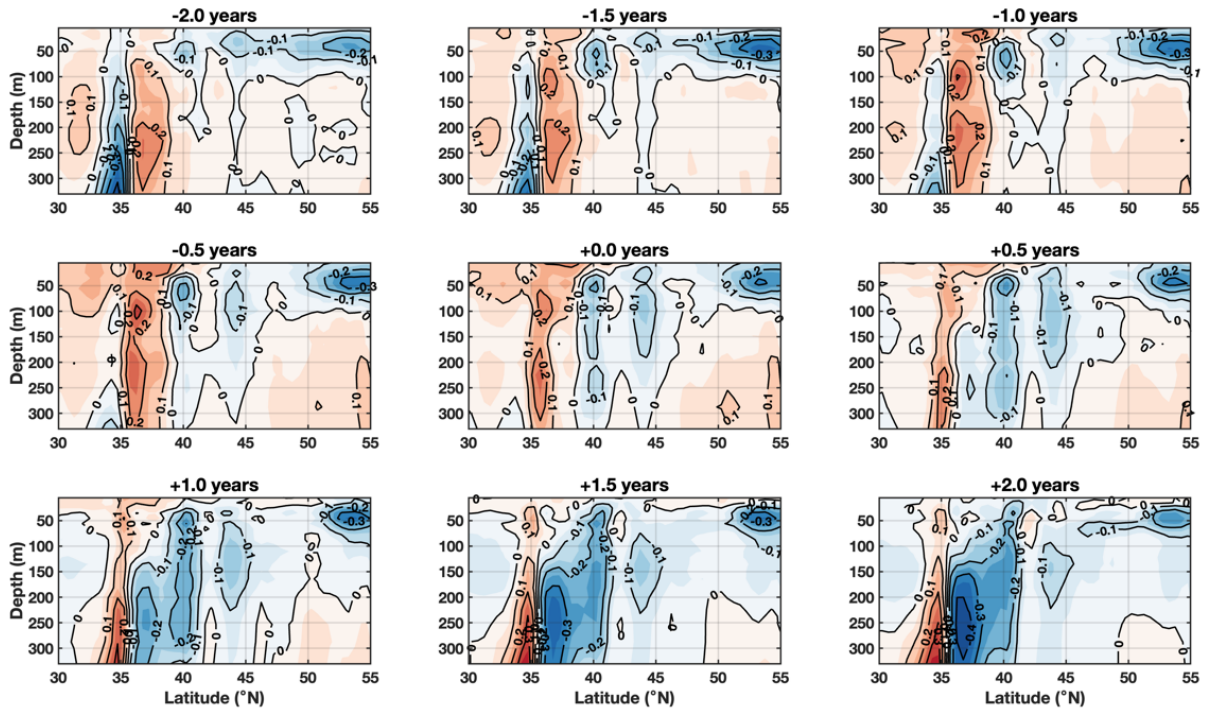
Supplementary figure 2. The normalized annual catch amounts of Pacific saury (black) and North Pacific Gyre Oscillation (NPGO) with a 2-year lag applied (NPGO leads 2 years, red) during 1950–2022.



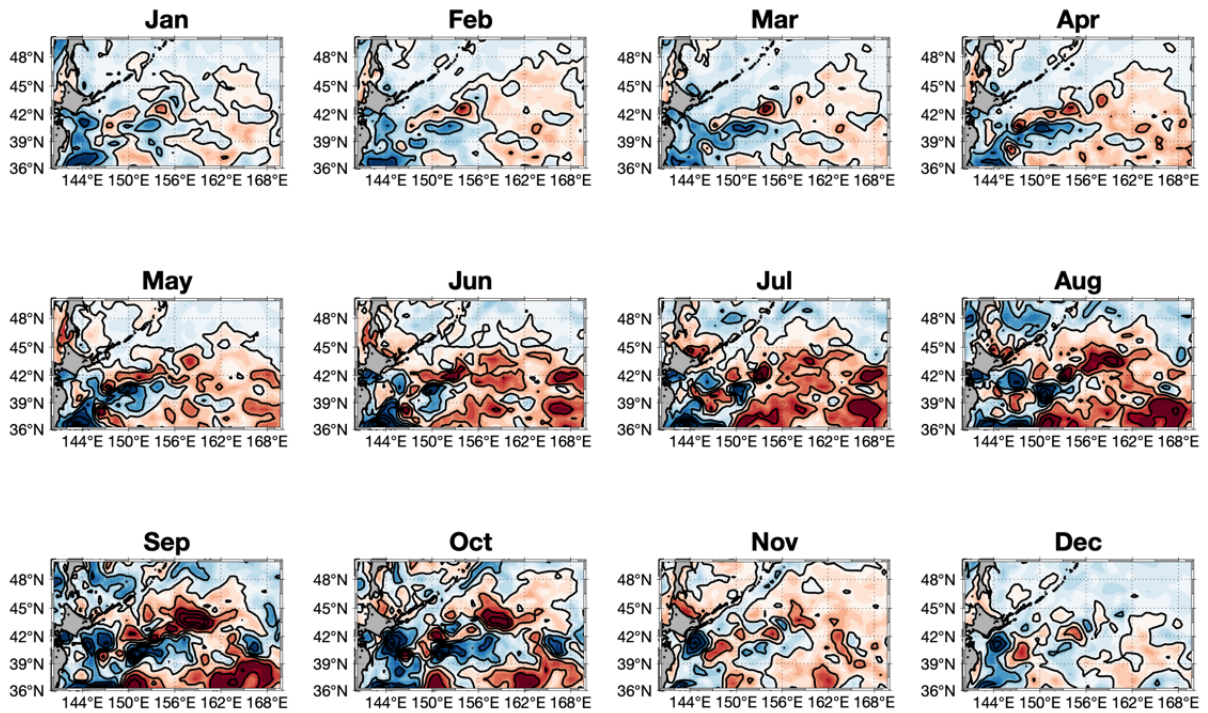
Supplementary figure 3. The monthly regressed and reconstructed temperature anomaly at 45 m depth in the North Pacific onto the annual catch amounts of Pacific saury during 1990–2020 (contour intervals: 0.2°C). Areas of positive temperature anomalies are shaded red, and areas of negative anomalies are shaded blue.



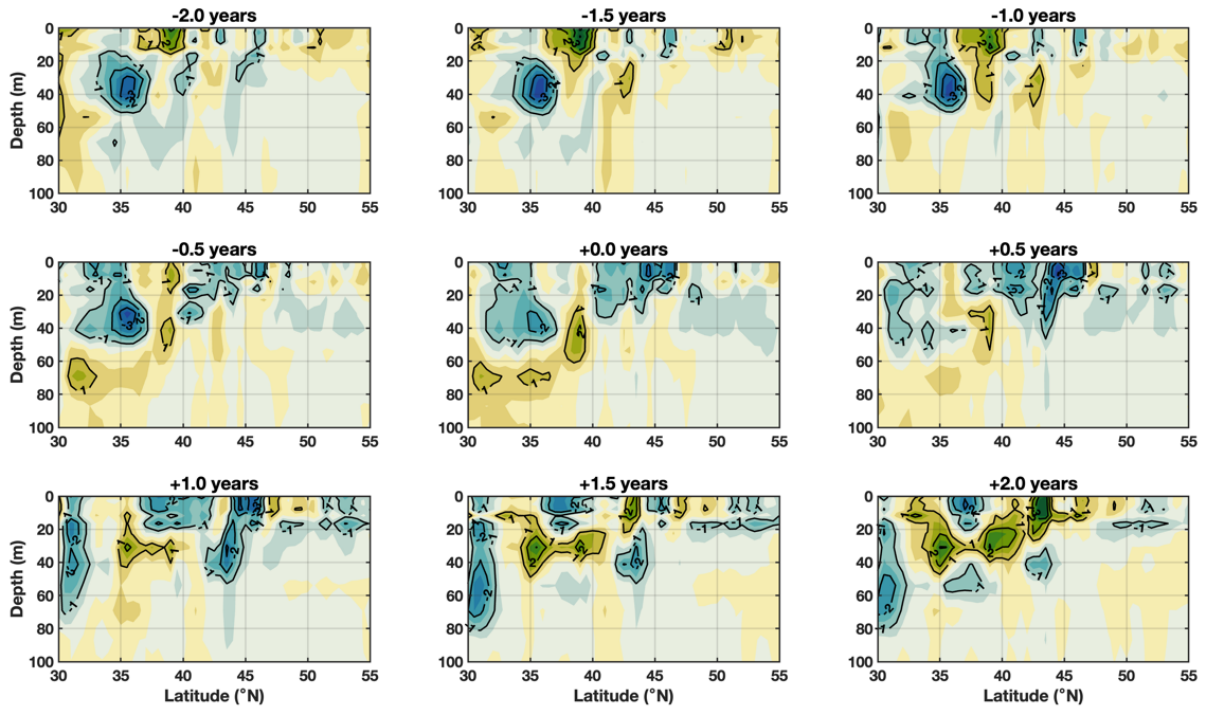
Supplementary figure 4. same as Supplementary figure 3, but for the net primary production during 1993–2020 (contour intervals: 0.5 mg/m³/day). Areas of positive anomalies are shaded green, and areas of negative anomalies are shaded blue.



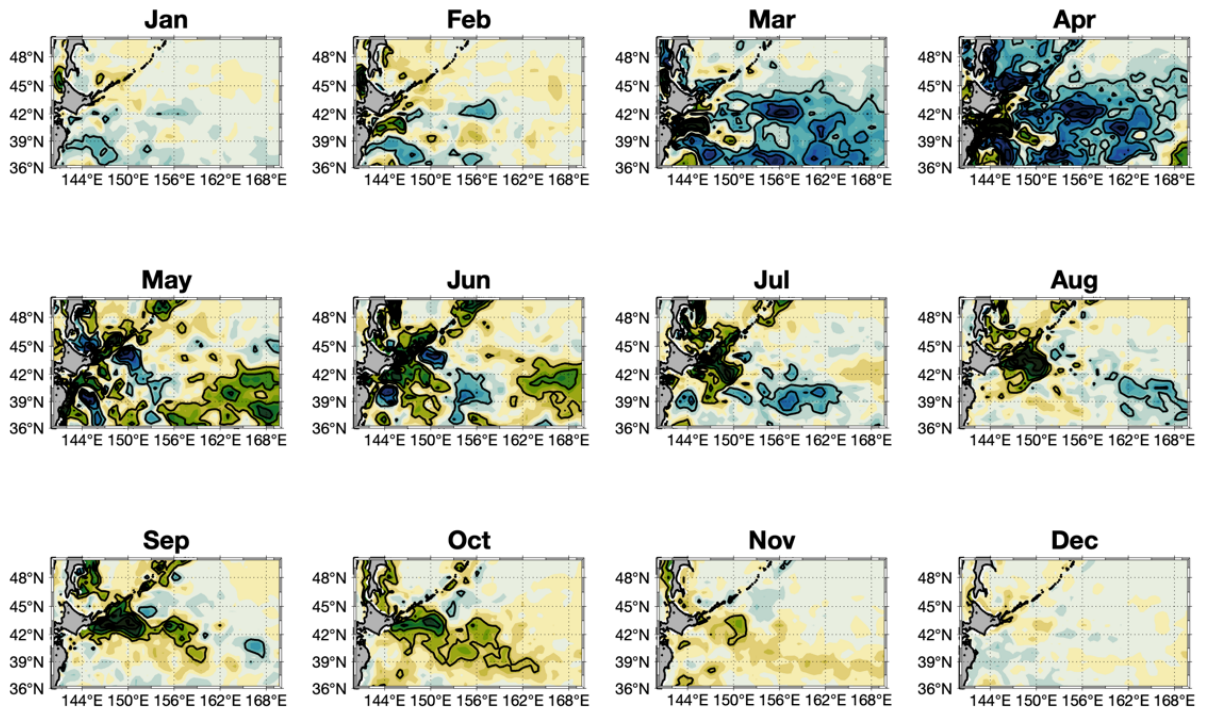
Supplementary figure 5. The zonally averaged (145–155° E) regressed and reconstructed upper 300 m temperature anomalies in the North Pacific onto the normalized 2-year low-pass filtered North Pacific Gyre Oscillation (NPGO) index. The target index is for 1990–2018, and temperature anomalies are for 1988–2020, with a time lag of ± 2 years. Numbers in the title indicate the time lags, and positive values indicate that the NPGO leads the temperature.



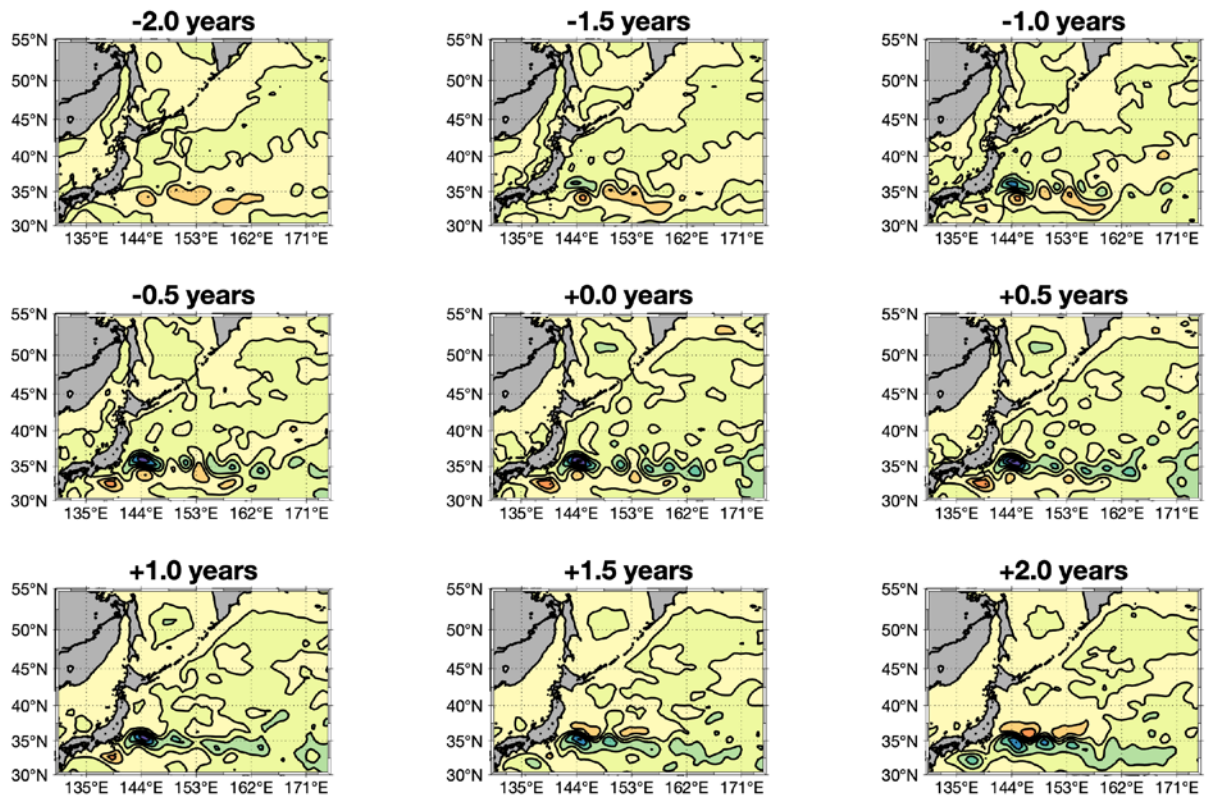
Supplementary figure 6. same as Supplementary figure 3, but for the North Pacific Gyre Oscillation (NPGO) with a 2-year lag (the NPGO leads by 2 years).



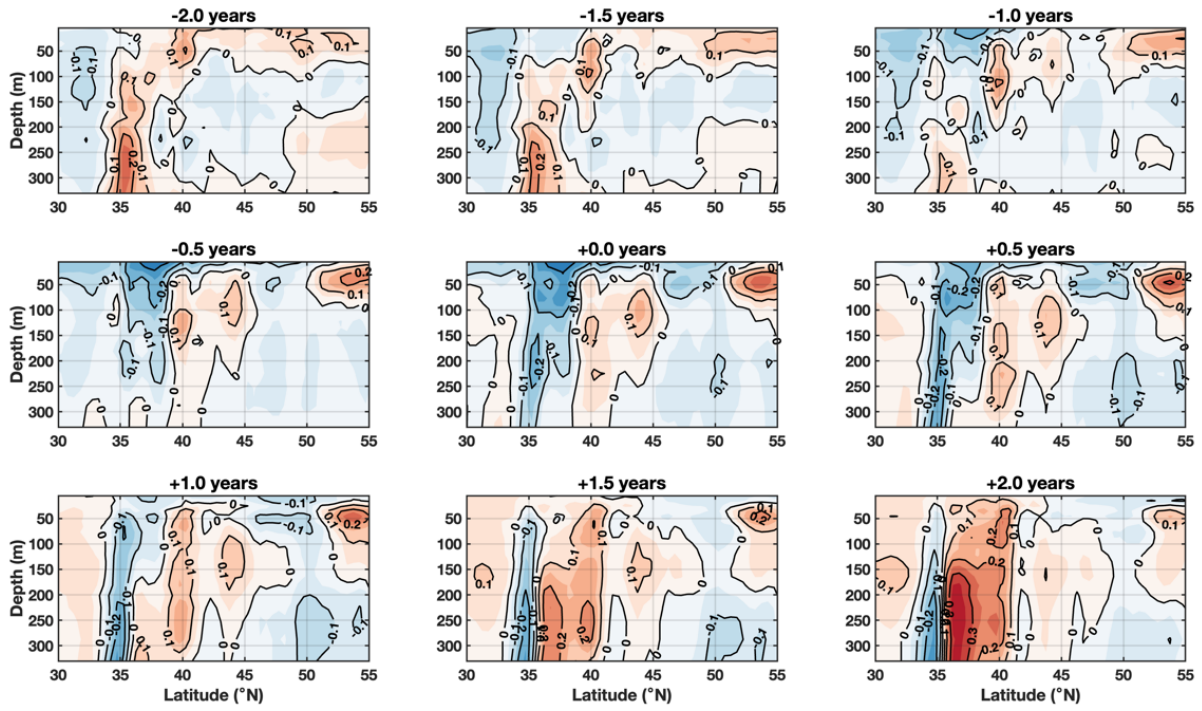
Supplementary figure 7. Same as supplementary figure 5, but for the net primary production during 1995–2020.



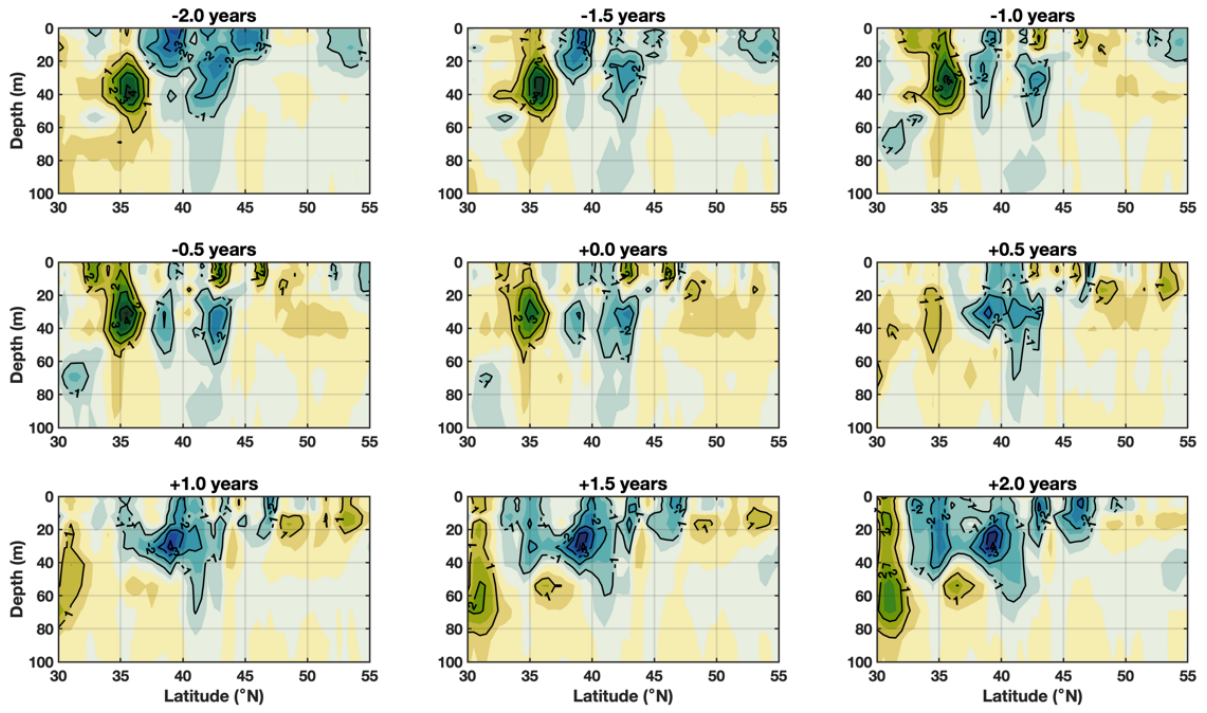
Supplementary figure 8. same as Supplementary figure 4, but for the North Pacific Gyre Oscillation (NPGO) with a 2-year lag (the NPGO leads by 2 years).



Supplementary figure 9. The regressed and reconstructed sea surface height (SSH) anomalies in the North Pacific onto the normalized 2-year low-pass filtered Pacific Decadal Oscillation (PDO) index (contour intervals: 2 cm). The target index is for 1990–2018, and the SSH anomalies are for 1988–2020, with a time lag of ± 2 years. Numbers in the title indicate the time lags and positive values indicate that the PDO leads the SSH. Areas of positive SSH anomalies are shaded red, and areas of negative anomalies are shaded blue.



Supplementary figure 10. same as supplementary figure 5, but for the 2-year low-pass filtered Pacific Decadal Oscillation Index.



Supplementary figure 11. same as supplementary figure 7, but for the 2-year low-pass filtered Pacific Decadal Oscillation Index.